Journal of Medicinal Chemistry

Article

pubs.acs.org/jmc

Differential Interactions of Rifabutin with Human and Bacterial Membranes: Implication for Its Therapeutic and Toxic Effects

Marina Pinheiro,[†] Mariana Arêde,[†] Cláudia Nunes,[†] João M. Caio,[‡] Cristina Moiteiro,[‡] Marlene Lúcio,[†] and Salette Reis*[,†]

[†]REQUIMTE, Departamento de Ciências Químicas, Faculdade de Farmácia, Universidade do Porto, Rua de Jorge Viterbo Ferreira no. 228, Porto 4050-313, Portugal

[‡]Centro de Química e Bioquímica, Departamento de Química e Bioquímica, Faculdade de Ciências, Universidade de Lisboa, Lisboa, Portugal

ABSTRACT: This work focuses on the interaction of rifabutin (RFB), a naphthalenic ansamycin, with membrane models. Since the therapeutic and toxic effects of this class of drugs are strongly influenced by their lipid affinity, we concerned specifically on the ability of this antibiotic to affect the membrane biophysical properties. The extent of the interaction between RFB and membrane phospholipids was quantified by the partition coefficient (K_p), using membrane model systems that mimic the human (liposomes of 1,2-dimyristoyl-*sn*-glycero-phosphocholine, DMPC) and the bacterial (liposomes of 1,2-dimyristoyl-*sn*-glycero-3-phosphoglycerol, DMPG) plasma membranes. To predict the drug location in the membranes, fluorescence quenching and lifetime measurements were carried out using the above-mentioned membrane models labeled with fluorescent probes. Steady-state anisotropy measurements were also performed to evaluate the effect of RFB on the microviscosity of the membranes. Overall, the results support that RFB has higher affinity for the bacterial membrane mediated by electrostatic interactions with the phospholipid head groups.

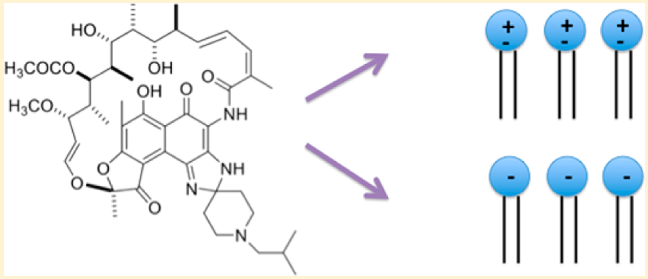

INTRODUCTION

Rifabutin (RFB, Figure 1), a naphthalenic ansamycin, is commonly used for the treatment of mycobacterial infectious diseases.[1] This semisynthetic derivate of rifamycin, which was approved in 1992 by the FDA, represents one of the most efficient antibiotics used in the tuberculosis (TB) treatment, being frequently used in HIV coinfected patients because of the fewer drug interactions with antiretroviral agents compared with rifampicin (a rifamycin first-line anti-TB drug).[2] Additionally, RFB is also used to treat atypical mycobacterial infections and, in some cases, it has shown to be active when resistance to rifampicin is found.[3,4] Although RFB is generally well-tolerated, there are some problematic side effects which include uveitis, rash, nausea, vomiting, neutropenia, anemia, discoloration of the skin and body fluids (tears, saliva, urine and perspiration), and, rarely, clinically important impairment of the liver function.[5] The accepted mechanism of action of RFB involves the binding to the β-subunit of the RNA polymerase, causing the inhibition of the RNA transcription and consequently the inhibition of the bacterial protein synthesis.[2] The binding constants for prokaryotic RNA polymerases are 10000-fold higher than those for eukaryotic enzymes, which in part might explain the higher selectivity of this drug to the bacteria and its usefulness in the TB therapy. Nevertheless, a lack of correlation has been found between the RFB inhibitory activity on the RNA polymerase and the antibiotic efficacy. Recently, it has been established that the drug's penetration through the bacteria cells explains the higher activity against Gram-positive compared to the Gram-negative despite the quite similar RNA polymerase inhibitory activities.[1] Indeed, the efficiency of the interactions of the antibiotics with the membranes constitutes one of the most important pharmacological features, playing an essential role on its biological activity.[6] RFB has an intracellular target, and hence it must pass across phospholipid bilayers to reach the RNA polymerase and elicit its pharmacological effect. There are several analogues of RFB described in the literature that were designed taking into consideration the binding to the RNA polymerase and which, despite being promising candidates, do not pass the preclinical trials.[2,7,8] In fact, the rational design of more efficient analogues of RFB against TB would benefit from a deeper understanding of the interactions of RFB with the human and bacterial membranes. Therefore, RFB was chosen in this study as a lead compound for new molecules as promising molecules against TB. For the purpose of this study, large unilamellar vesicles (LUVs) were used as lipid bilayer membrane models. As membrane models, liposomes take into account the RFB's passive diffusion across the bilayers. Nevertheless, the drugs permeation through the membranes involves other processes,

Received: July 30, 2012
Published: December 10, 2012

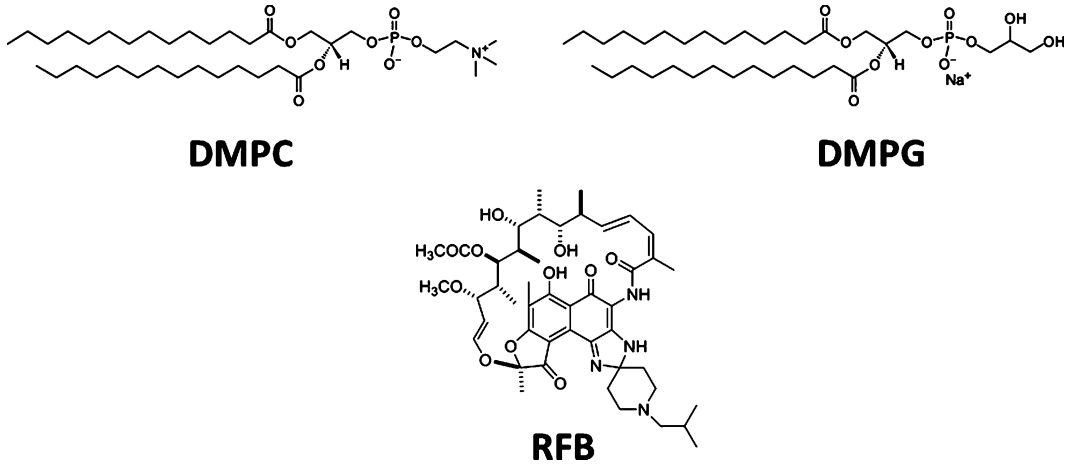

Figure 1. Molecular structures of 1,2-dimyristoyl-*sn*-glycero-phosphocholine (DMPC), 1,2-dimyristoyl-*sn*-glycero-3-phosphoglycerol (DMPG), and Rifabutin (RFB).

namely the paracellular diffusion through the cell junctions and the active transport that leads to the influx and efflux of drugs facilitated by transport proteins.[9] Because of its high lipophilicity, the passive diffusion is probably the most relevant process of the RFB's permeation through the membranes. Regarding the lipophilicity of RFB, its plasma concentrations do not reflect the concentrations that can be achieved in target organs and infected cells. Therefore, RFB penetrates well into polymorphonuclear leukocytes, lymphocytes, and macrophages, and it is well-known that it accumulates in organs as the lungs at levels six times higher compared with the plasma concentrations. Additionally, RFB is commonly used during prolonged periods and has a long half-life in the circulation.[10] Thus, because of the above-mentioned reasons the concentrations used in this work were significantly higher (approximately 25 times) compared with the plasma concentrations after a daily dose. Moreover, the range of RFB used was similar or even lower than that used in other similar studies when assessing the RFB−membrane models interactions.[11,12] Because phosphatidylcholines are practically absent in bacterial plasma membranes and are generally the most abundant phospholipids in eukaryotic plasma membranes, DMPC (Figure 1), a zwitterionic lipid, was chosen to mimic the human plasma membrane.[13,14] For these reasons, DMPC constitutes a suitable model for the surface membrane of mammalian cells and mimics the neutral charge of the host human plasma membrane. On the other hand, phosphatidylglycerols are almost absent in eukaryotic plasma membranes but are ubiquitous and often abundant in bacterial plasma membranes. Hence, DMPG (Figure 1), a negatively charged lipid, may be considered an adequate model for the mycobacterial membrane by mimicking the phospholipid negative charge of the inner plasma membrane of the Gram-positive bacteria (that includes the *Mycobacterium* spp.).[13,15] In fact, one of the main differences between Gram-positive and Gram-negative bacteria is the lipid composition of its membranes. Despite the wide variation in the phospholipid composition, while plasma membranes of Gram-positive bacteria predominantly contain anionic lipids, plasma membranes of Gram-negative bacteria contain both anionic and zwitterionic lipids.[16]

The knowledge concerning the biophysical interactions of RFB with the membrane lipid bilayer is scarce, in particular the information regarding the penetration into membranes of different phospholipid constitution. Previous works reported the higher preference of RFB for negatively charged membrane models.[11,12,17] Vostrikov and co-workers[12] determined the distribution coefficient of RFB by fluorescence quenching using LUVs of PC and PC:cardiolipin (CL) and concluded that RFB might establish electrostatic interactions with the membranes due to the higher distribution obtained in the negatively charged model. Using phase separation and fluorescence quenching, Vostrikov and colleagues determined the distribution coefficient of RFB and proved that the insertion of a CL in PC multilamellar liposomes (MLVs) increases the binding of RFB to the lipid bilayer. Results obtained by ^{31}P NMR spectroscopy have shown that despite RFB penetrating the membrane, it does not alter the bilayer structure of the membrane models studied.[11]

The main purpose of this work is to study the effect of RFB on the different nature head group phospholipids, evaluate the putative differential RFB interactions with human and bacterial membrane models, gain a higher knowledge about the RFB's location and transport through the human and bacterial biomembranes, and understand if the drug induces changes in the biophysical properties of the lipid bilayer membranes. To assess the interaction between RFB and the membranes, several biophysical techniques were used. The partition of RFB between DMPC:aqueous and DMPG:aqueous phases was determined using derivative UV−Vis spectrophotometry. The fluorescence determinations were executed by monitoring the quenching of two probes, 1,6-diphenyl-1,3,5-hexatriene (DPH) and (2-carboxyethyl)-1,6-diphenyl-1,3,5-hexatriene (DPH-PA) in the RFB's presence. Fluorescence quenching was performed in order to obtain the drug location within the membrane lipid bilayers. Because the probe's location is well-known and the extent of the drug quenching is inversely proportional to its distance to the fluorophore, it is possible to estimate the drug's location within the membrane models.[18] To understand the biophysical modifications in the membrane's lipid bilayer induced by RFB molecules, steady-state anisotropy measurements were also employed. To our knowledge, this is the first report with the prevision of the RFB's location and its influence in the biophysical parameters of the human and bacterial membrane model systems.

The overall results allow us to conclude that RFB is able to permeate both membrane models. Notwithstanding, the ionic bonds are responsible for a higher affinity of RFB to the

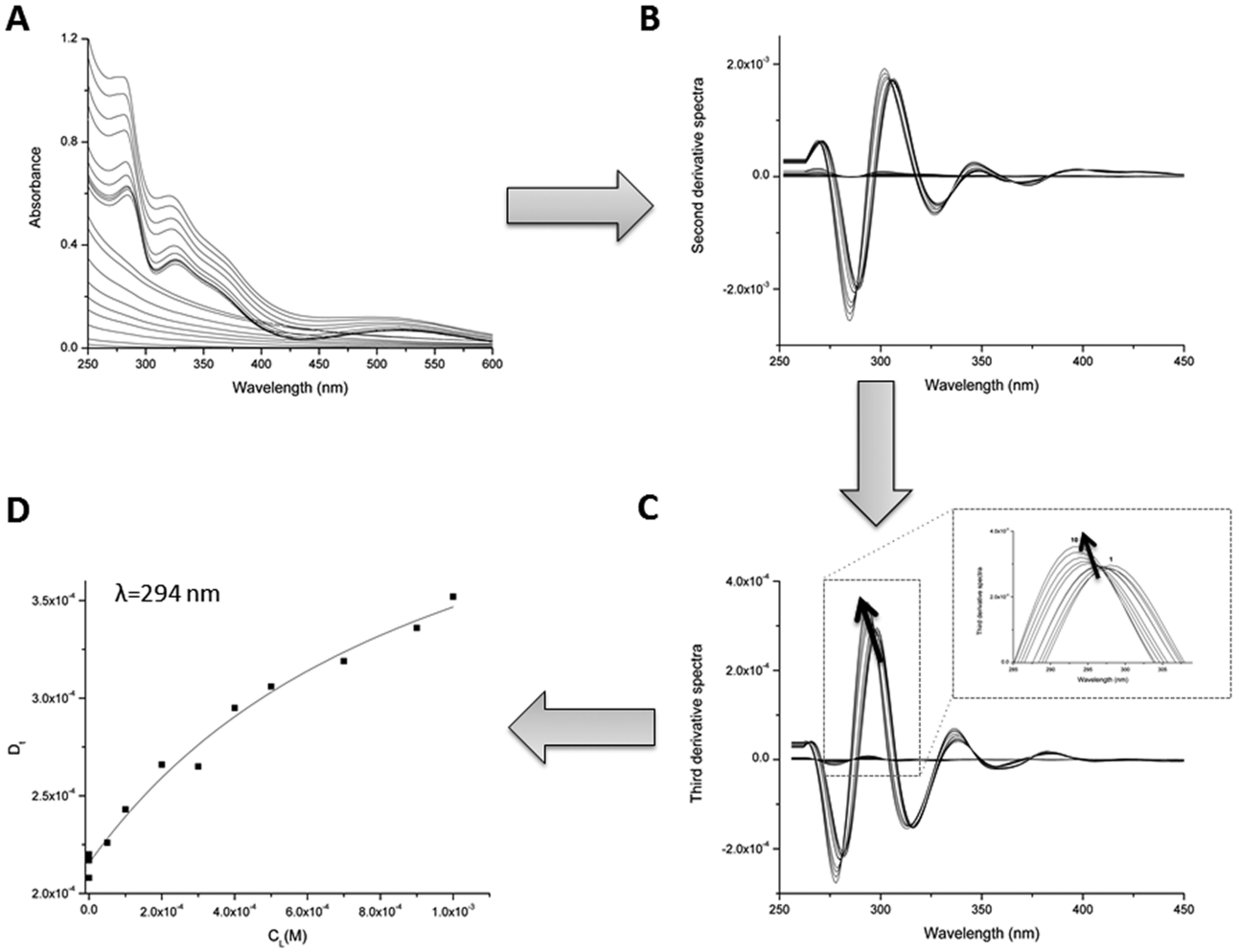

Figure 2. Absorption spectra (A), second derivative spectra (B), and third derivative spectra (C) of RFB (25 μM) incubated in LUVs of DMPC liposomes (black lines) and LUVs of DMPC liposomes without drug (gray lines) with different concentrations (M): (1) 0, (2) 5×10^{-5}, (3) 1×10^{-4}, (4) 2×10^{-4}, (5) 3×10^{-4}, (6) 4×10^{-4}, (7) 5×10^{-4}, (8) 7×10^{-4}, (9) 9×10^{-4}, (10) 1×10^{-3}. The curve (D) represents the best fit by eq 1 to experimental third derivative spectrophotometric data (D_t vs $[L]$) using a nonlinear least-squares regression method at wavelength 294 nm where the scattering is eliminated.

negatively charged membrane model. Regarding this, the mechanism by which this antibiotic permeates through the phospholipid bilayers might include an electrostatic adsorption at the interface region, followed by its permeation and induction of pronounced changes into the bacterial membrane biophysics.

In summary, this work contributes to identify novel biophysical mechanisms that may permit to explain the toxic and therapeutic effects of RFB and that might allow the future development of more effective anti-TB drugs.

RESULTS AND DISCUSSION

Partition of RFB on DMPC and DPMG Liposome-Based Membrane Mimetic Systems. The lipophilicity of drug molecules (normally represented as the logarithm of the *n*-octanol:water partition coefficient, log *P*) often strongly correlates with their pharmacological activity.[19] Thus, the lipophilicity is an important property of an antibacterial agent and should increase its efficacy, especially in the *Mycobacterium* spp. Indeed, the intrinsic permeability of the lipid domain of the mycobacterial cell wall is so low that an increment in the lipophilicity is expected to increase the extent of penetration and hence the efficacy of the antibiotics.[20]

The determination of the lipophilicity of ionizable compounds, which is normally represented by the distribution coefficient (log *D*), is often misleading, with some variability in the results according to the different techniques. The RFB molecule contains some groups that can undergo protonation (piperidine nitrogen, pK_a 9.5 and imidazole nitrogen, pK_a 3.5) and deprotonation (naphthol oxygen, pK_a 6.5). At the physiological pH, while zwitterionic species predominate (83.4%), cations make up 16.6% (predicted using a chemical software).[11] Because of the RFB ionization at the physiological pH and in order to evaluate the different interactions that occur between the drug and the bacterial plasma membrane and between the drug and host plasma membrane, we have chosen a liposome:aqueous system instead of the classical biphasic *n*-octanol:aqueous system. In fact, because of their structural and anisotropic environment similar to the biomembranes, liposomes constitute a more realistic analytical system and can better mimic the cell membranes, providing additional information to that obtained with the *n*-octanol:aqueous system.[14] The K_p, expressed in terms of log *D*, was obtained by derivative UV–Vis spectrophotometry. This spectroscopic technique, due to its sensitivity, allows straightforward procedures and the possibility to analyze signals originated

dx.doi.org/10.1021/jm301116j | J. Med. Chem. 2013, 56, 417–426

from both lipid and aqueous phases without the need to apply separation procedures.[14] Derivative spectrophotometry eliminates the intense background signals arising from the light scattered by lipid vesicles and improves the resolution of overlapping bands, features that have been reported by several authors.[18,21] The partition coefficients were calculated from the second and third derivative spectra (determined from the recorded absorption spectra after blank subtraction) at the wavelengths where the scattering is eliminated, by fitting eq 1 to the experimental data (D_t versus $[L]$) using a nonlinear least-squares regression method where the adjustable parameter is the partition constant, K_p:[14,21]

$$D_T = D_w + \frac{(D_m - D_w)K_p[L]V_m}{1 + K_p[L]V_m} \quad (1)$$

In this equation, D is the second or the third derivative intensity ($D = (d^nAbs)/(d\lambda^n)$) obtained from the absorbance values of the total concentration of RFB (D_T), RFB distributed on the lipid membrane phase (D_m), and RFB distributed in the aqueous phase (D_w); $[L]$ is the lipid concentration and V_m is the lipid molar volume. For DMPC and DMPG, the values of V_m are respectively 0.66 and 0.67 L mol^{-1} (calculated from the mean molecular weight and the reported specific volume of lipids).[14]

The absorption and the second and the third derivative spectra for RFB containing different concentrations of LUVs composed of DMPC are shown in Figure 2. The λ of the maximum absorption of RFB in DMPC (Figure 2D) and DMPG (not shown) exhibits a hypsochromic shift (of 4 nm) in accordance to the increase in the lipids concentration, indicating the partition of the drug to the lipid bilayers.[21] Figure 2D shows, as an example, the best fit of the eq 1 to the third derivative spectrophotometric data collected at λ = 294 nm for RFB with different concentrations of DMPC liposomes.

The values of the K_p of RFB, expressed as log D, between lipids (LUVs of DMPC and DMPG) and the buffer system are listed in the Table 1.

Table 1. Partition Coefficients (log D) (Dimensionless) for RFB in DMPC and DMPG Liposomes (500 μM, T = 37.0 ± 0.1 °C pH 7.4) Obtained in the Fluid Phase[a]

	DMPC:aqueous	DMPG:aqueous
log D	3.0 ± 0.1	3.6 ± 0.1

[a]Results present the mean and standard deviation of at least three independent assays.

The analysis of the obtained log D values reveals that RFB exhibits a higher partition for the DMPG liposomes. At the physiological pH, the contribution of the positively charged molecules (due to the ionization of the piperidine nitrogen) might be responsible for this higher partition due to the electrostatic interactions with the polar head groups of DMPG liposomes.

The predicted log P and log D, obtained using the chemical software, were respectively 4.57 and 3.06. The predicted log P is clearly higher because it does not account the occurrence of modifications in the hydrophobicity of ionizable compounds at varying pH. Contrastingly, the predicted log D is in close agreement with the experimental partition of RFB obtained for DMPC liposomes. Therefore, hydrophobic interactions are expected to be the main interactions occurring with the zwitterionic lipid membranes. Furthermore, the higher log D obtained for DMPG confirms that not only hydrophobic intermolecular forces drive the drug's partition. Therefore, the RFB's interaction with DMPG also encodes ionic bonds between the protonated imidazole and piperidine nitrogen and the deprotonated phosphate from the phospholipid head groups.[22]

Studies of RFB Location in the Lipid Bilayer of Membrane Mimetic Systems. Fluorescence quenching is a sensitive method that has long been used to study the location of specific ligands within liposomes and biological membranes.[23] The membrane location of RFB was assessed by fluorescence quenching measurements using two fluorescent probes (DPH and DPH-PA). When the probes are included in the lipid bilayer, the precise fluorophore positions along the membrane depth plane are well-established and documented.[24,25] While DPH-PA probe is anchored to the surface of the membrane in the phospholipids polar head groups,[24,26,27] the DPH probe has a deeper location and a parallel alignment to the acyl chains.[24−26] A huge variety of molecular interactions can result in the decrease of the fluorescence intensity of a sample (process called quenching). Because it is the most appropriate method to distinguish the type of quenching (static or dynamic), not only the intensity of the fluorescence emission was measured but also the fluorescence lifetimes.[23] Moreover, to definitely prove the type of fluorescence quenching the studies were performed at several temperatures.[28] The collisional quenching of fluorescence is described by the Stern−Volmer equation (eq 2):[23]

$$\frac{I_0}{I} = 1 + K_{SV}[Q]_m = \frac{\tau_0}{\tau} \quad (2)$$

In this equation, I_0 and I are respectively the fluorescence intensities in the absence and presence of the quencher; K_{SV} is the quenching constant, called the Stern−Volmer constant; τ_0 and τ are the lifetime of the fluorophore in the absence and presence of the quencher; $[Q]_m$ is the concentration of the quencher that is able to partition the membrane, which is calculated from the total drug concentration ($[Q]_T$) and from the drug's partition coefficient (K_p), as described by the following equation:[23]

$$[Q]_m = \frac{K_p[Q]_T}{K_p\alpha_m + (1 - \alpha_m)} \quad (3)$$

where α_m is the volume fraction of the membrane phase ($\alpha_m = V_m/V_T$; V_m and V_T represent respectively the volumes of the membrane and water phases). The Stern−Volmer equation (eq 2) illustrates an important characteristic of the collisional quenching, which is an equivalent decrease in the fluorescence intensity and lifetime. If the quenching is purely collisional, $I_0/I - 1$ is expected to be linearly dependent upon the concentration of the quencher. In several instances, the fluorophore can be quenched both by collisions and by complex formation with the same quencher, being an upward curvature of the Stern−Volmer plot a characteristic feature in these circumstances. The dynamic portion of the observed quenching is determined by lifetime measurements using the following equation, $\tau_0/\tau = 1 + K_D[Q]$. So, by knowing the dynamic component, the static contribution may be found by linearization of the following equation (eq 4):

dx.doi.org/10.1021/jm301116j | J. Med. Chem. 2013, 56, 417−426

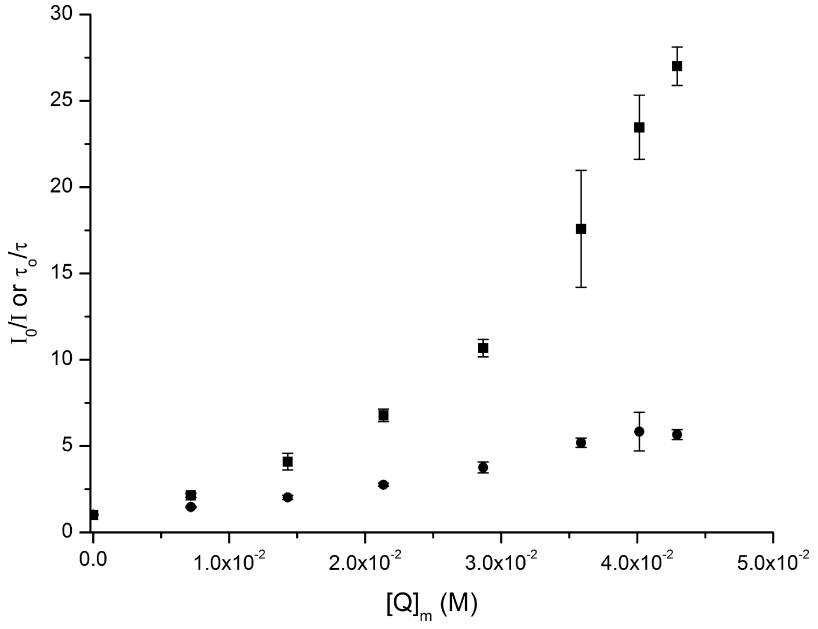

Figure 3. Stern–Volmer plots of the probe DPH-PA in LUVs of DMPG (500 μM, T = 37.0 ± 0.1 °C pH 7.4) by increasing concentrations (M) of the quencher RFB. The squares (■) represent Stern–Volmer plot obtained by steady-state fluorescence measurements (I_0/I), and circles (●) represent Stern–Volmer plot obtained by lifetime fluorescence measurements (τ_0/τ).

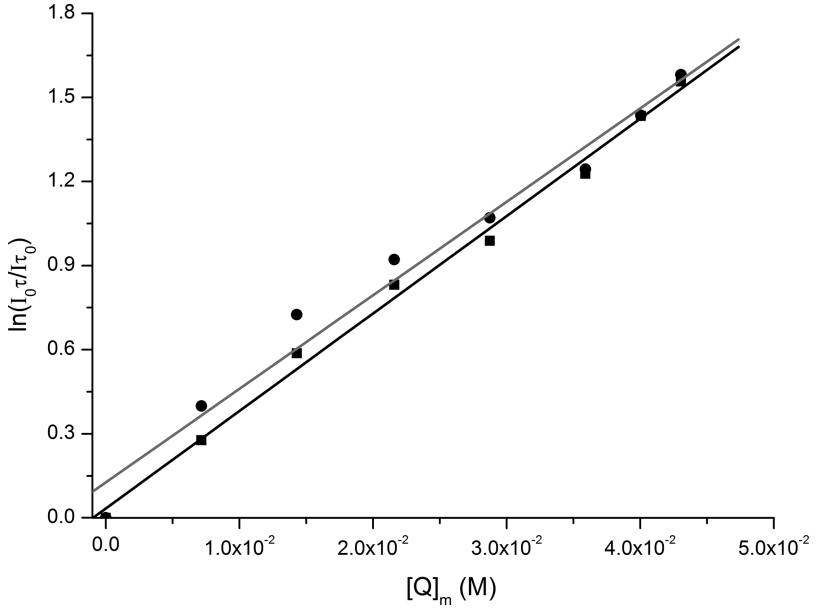

Figure 4. Fluorescence quenching of DPH (■) and DPH-PA (●) probes in LUVs of DMPG (500 μM, T = 37.0 ± 0.1 °C pH 7.4) by increasing concentrations of RFB and respective application of the mathematical model "sphere of action". Lines represent fits to eq 5.

$$\frac{I_0}{I} \times \frac{1}{1 + K_D[Q]_m} = 1 + K_S[Q]_m \quad (4)$$

This modified form of the Stern–Volmer equation is second order in $[Q]_m$, which accounts for the upward curvature observed when both static and dynamic quenching occur for the same fluorophore. In the Figure 3, the Stern–Volmer plots of I_0/I against $[Q]_m$ and τ_0/τ against $[Q]_m$ are depicted. From the Figure 3, it may be concluded that the quenching is not purely collisional and might also be due to the formation of a static quenching process. As a result, RFB must diffuse to the fluorophore during the lifetime of the excited state. After the contact, the fluorescent probe returns to the ground state without the photon emission. Moreover the static quenching is also present and the fluorophore and RFB form a non-fluorescent complex.[23,28]

Nevertheless, the positive deviation of the Stern–Volmer plots can also be interpreted in terms of a "sphere of action" static quenching model. According to this model, instantaneous quenching occurs if the quencher molecule is adjacent to the fluorophore at the moment of excitation. When the fluorophore and quencher are in such proximity, there is a high probability that quenching will occur before these molecules diffuse apart. As the quencher concentration increases this probability also increases because the quencher is within the "sphere of action" of the fluorophore at the moment of excitation. Hence, only a

dx.doi.org/10.1021/jm301116j | J. Med. Chem. 2013, 56, 417–426

Table 2. Values of Stern–Volmer Constant at T = 37.0 ± 0.1 °C (K_{SV}) and 42.0 ± 0.1 °C (K_{SV}*) and Bimolecular Quenching Constant (K_q) Obtained for RFB in DMPC and DMPG Liposomes (500 μM, T = 37.0 ± 0.1 °C pH 7.4) Labeled with DPH or DPH-PA Probes

	K_{SV} (M^{-1})		K_{SV}* (M^{-1})		K_q (M^{-1} s^{-1})	
	DPH	DPH-PA	DPH	DPH-PA	DPH	DPH-PA
DMPC	216 ± 10	165 ± 10	156 ± 14	76 ± 9	27 ± 1	29 ± 2
DMPG	167 ± 13	181 ± 10	132 ± 8	121 ± 9	19 ± 1	26 ± 1

certain fraction of the excited fluorophore is quenched by the Stern–Volmer collisional mechanism. Moreover, this model assumes that if the quencher is located inside a spherical volume (V) adjacent to the fluorophore, the probability for the quencher to be inside this volume at the time of excitation depends on the volume itself and on the quencher concentration ($[Q]_m$), as it is described by the modified Stern–Volmer equation (eq 5):[23]

$$\ln\left(\frac{I_0\tau}{I\tau_0}\right) = V[Q]_m \tag{5}$$

For both membrane models, the data was treated according to the "sphere of action" quenching model and is represented in the Figure 4. The analyses of the Figure 4 permit the conclusion that the results obtained in this work are in good agreement with the "sphere of action" quenching model.

The bimolecular quenching constant (K_q) is a fundamental parameter that reflects the efficiency of quenching or the accessibility of the probes to the drug and is calculated as follows (eq 6):[23]

$$K_q = \frac{K_{SV}}{\tau_0} \tag{6}$$

The K_{SV} values at two different temperatures and the K_q as the sum of both contributions (static and dynamic) are listed in the Table 2. The results suggest that for both membrane models the quenching process is the result of dynamic and static interactions with a dominant static component. The K_{SV} values decrease with the increase of temperature (from 37.0 to 42.0 °C), which is indicative of a nonfluorescence complex dissociation and a confirmation that the static quenching is present. The location studies have shown that in DMPG liposomes, the quenching efficiency of the DPH-PA is higher than that of DPH. This is in accordance with the preferential location of RFB near the polar region of the negatively charged phospholipids. The similar K_q values obtained for DPH and DPH-PA in the DMPC suggest that RFB does not have a preferential location in phospholipid membranes with no net charge. Hence, RFB in the zwitterionic membrane model is located in the surface as well as inside of the membrane hydrocarbon core. Moreover, the high values obtained for the DPH indicate that the drug is able to penetrate the bilayer in both lipids and especially in the DMPC. The molecules of RFB with no net charge should be inserted in the phospholipid bilayers according to their hydrophobicity gradient. The hydrophilic part of RFB, namely imidazole and piperidine moieties (Figure 1), should therefore be located near the head groups of the phospholipids and the hydrophobic naphthol must be embedded within the membrane, establishing van der Waals interactions with the phospholipid tails.[11] Moreover, the positively charged RFB seems to establish electrostatic interactions with the deprotonated phosphate group of the DMPG phospholipids. The electrostatic interactions appear to be less pronounced in the case of DMPC due to the presence of a protonated choline group in the head groups of the phospholipids that may cause electrostatic repulsions that hinder the partition of the positively charged drug.

Effects of RFB on the Microviscosity of the Membrane Mimetic Systems. Steady-state fluorescence anisotropy measurements have been widely used to quantify the fluidity gradient across bilayer structures and the results obtained have proven to be consistent with a variety of other physical techniques.[13] To study the influence of the RFB on the fluidity of the membranes, cell-based assays and the parallel artificial membrane permeability assay (PAMPA) could also have been performed. However, these techniques do not allow to fully understanding how RFB affects the biophysical parameters of the membrane models used.[29] Furthermore, to complement the information provided by the quenching data, steady-state fluorescence anisotropy was carried out to study the effect of RFB on the membrane lipids main phase transition temperature (T_m) and, accordingly, extrapolate the influence of this compound on the bacterial and human host plasma membrane microviscosity. The fluorescence steady-state anisotropy (r_s) is defined by the following equation (eq 7):[21,30]

$$r_s = \frac{I_{VV} - I_{VH}G}{I_{VV} + 2I_{VH}G} \tag{7}$$

where I_{VV} and I_{VH} are the polarized intensities measured in directions parallel and perpendicular to the excitation beam. The correction factor ($G = I_{HV}/I_{HH}$) is the ratio of the detection system sensitivity for vertically and horizontally polarized light, which is given by the ratio of vertical to horizontal components when the excitation light is polarized in the horizontal direction.[30] The temperature dependence of the DPH fluorescence anisotropy in the absence and presence of RFB is shown for DMPC and DMPG liposomes, respectively, in Figure 5A and 5B. From the experimental data displayed, it is possible to calculate the cooperativity (B) and the T_m, which corresponds to the temperature of the gel-to-fluid phase transition of DMPC and DMPG and is calculated from the inflection point of the data fitted to sigmoid curves of steady-state anisotropy (r_s) versus temperature (T) (eq 8):

$$r_s = r_{s1} + p_1T + \frac{r_{s2} - r_{s1} + p_2T - p_1T}{1 + 10^{B(1/T - 1/T_m)}} \tag{8}$$

where p_1 and p_2 correspond to the slopes of the straight lines at the beginning and at the end of the plot and r_{s1} and r_{s2} are the respective steady-state anisotropy intercepting values at the y axis. The order parameter can also be calculated $s = (r_\infty/r_0)^{1/2}$, where r_0 (fundamental anisotropy) is the fluorescence anisotropy in absence of any rotational motion of the probe and r_∞ (limiting anisotropy) reflects the restriction of the probe motion.[21]

Besides analyzing the differences of RFB in its ability to disturb the DMPC and DMPG liposomes, it is important to

dx.doi.org/10.1021/jm301116j | J. Med. Chem. 2013, 56, 417–426

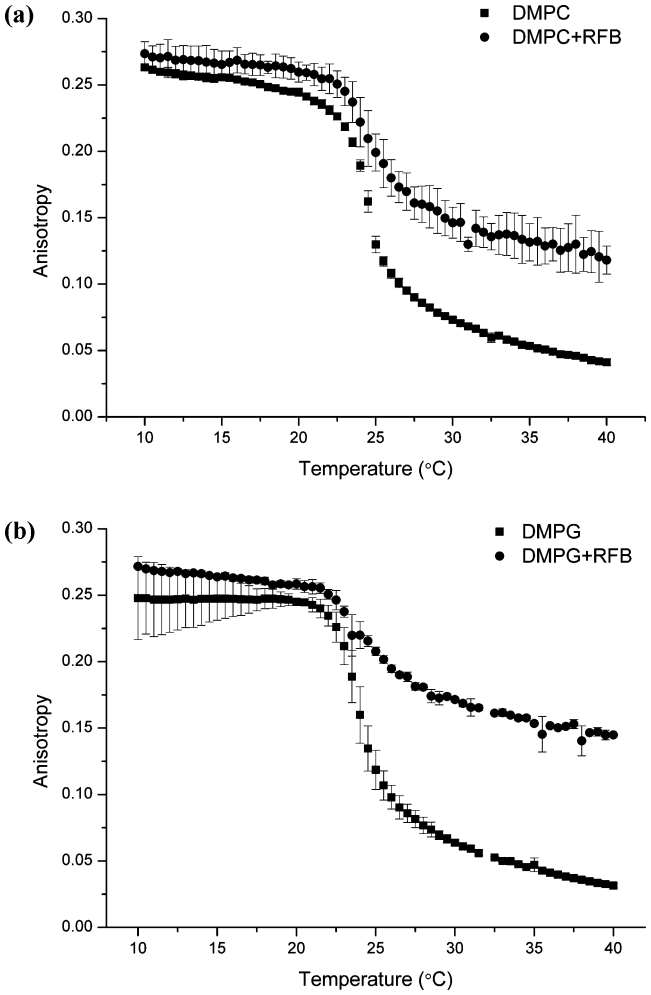

Figure 5. (A) Steady-state anisotropy of DPH in absence (■) and in the presence (●) of RFB (30 μM) in DMPC liposomes at pH = 7.4 as a function of temperature. Each point corresponds to the mean value of three experiments. Continuous lines are the best-fit curves using eq 8. (B) Steady-state anisotropy of DPH in absence (■) and in the presence (●) of RFB (30 μM) in DMPG liposomes at pH = 7.4 as a function of temperature. Each point corresponds to the mean value of three experiments. Continuous lines are the best-fit curves using eq 8.

compare the results obtained for DPH and DPH-PA, as they are located in different sites of the lipid bilayer and therefore report the microfluidity of those regions.[31] Moreover, regarding the previous results, RFB has already shown capacity to quench DPH and DPH-PA. The results presented in Table 3 for DMPC and DMPG using both probes show that the T_m values of DMPC and DMPG are consistent with the literature.[32,33] Independently of the probe, the T_m is not affected by the drug's presence in both models (Table 3). RFB penetrate both membrane models at temperatures above the T_m, taking into consideration the changes in the anisotropy when compared to the liposomes without drug (Figure 5). This is in accordance with the bulky structure of RFB and its relative rigid structure, being the highly ordered state of the lipids a hindrance to the drug's penetration.[11,12] Additionally, at temperatures above the T_m, RFB is responsible for higher values of anisotropy in both models compared to the liposomes alone. The higher values of anisotropy indicate that the drug decreases the fluidity of the membrane models (Figure 5). The decrease in the membrane fluidity due to the RFB's presence is more pronounced for the DMPG liposomes. In contrast to the T_m, at the fluid phase the cooperativity and the degree of molecular packing (order) significantly change with the drug's presence (Table 3). The drug decreases the cooperativity of the phase transitions and increases the order of both lipids, which confirms that RFB penetrates both membrane models. Moreover, RFB changed the cooperativity and the order (Table 3), especially in the DMPG, meaning that in this model, the drug must be located closer to the more ordered region, namely in the vicinity of the head groups of the phospholipids (correspondent to the acyl chains from C1 to C8 region).[34,35] Therefore, the increment in the DMPG order may be caused by the electrostatic interactions between RFB and the phospholipid head groups, with a consequent screening of the negative surface charge that might decrease the repulsive forces between the phospholipid head groups. Again, these results are consistent with the above-mentioned prevision of the drug's location.

CONCLUSION

Antibiotic-mediated bacterial cell death is a complex process that begins with the biophysical interaction between the drugs and the biomembranes.[36,37] Thus, to reach its intracellular target (bacterial RNA polymerase), RFB must pass across the human plasma membranes (absorption/distribution) and thereafter the mycobacterial plasma membranes (generally inside the human macrophages). Notwithstanding the binding to the RNA polymerase, the mechanism of action of RFB seems to be much more multifaceted and might be related to the drug's lipid affinity. The results revealed that the surface charge of the phospholipids played a major role in the differential interactions of RFB with membranes. The determination of the partition coefficient showed a higher value for the DMPG:aqueous compared to the DMPC:aqueous liposomes, suggesting that the partition of the drug depends on the lipid's charge and it is regulated by electrostatic interactions. The higher partition of the drug for the mycobacterial membrane model is in agreement with the higher affinity of RFB to the membranes with negatively charged lipids, which result in a higher selectivity and higher RFB concentrations that reach the

Table 3. Values of Main Phase Transition Temperature (T_m), Cooperativity (B), and Order Parameter (S) Obtained for DMPC and DMPG Liposomes (500 μM, T = 37.0 ± 0.1 °C pH 7.4) Labeled with DPH or DPH-PA Probes in the Absence and in the Presence of RFB (30 μM)

	DPH			DPH-PA		
	T_m (°C)	cooperativity (B)	order (S)	T_m (°C)	cooperativity (B)	order (S)
DMPC	24.4 ± 0.2	347 ± 34	0.39 ± 0.04	24.6 ± 0.3	246 ± 27	0.66 ± 0.02
DMPC+RFB	24.5 ± 0.8	254 ± 35	0.63 ± 0.03	24.5 ± 0.4	214 ± 23	0.73 ± 0.03
DMPG	24.1 ± 0.5	233 ± 5	0.34 ± 0.03	23.9 ± 0.3	354 ± 37	0.75 ± 0.02
DMPG+RFB	24.4 ± 0.3	182 ± 34	0.66 ± 0.02	24.2 ± 0.7	209 ± 28	0.85 ± 0.02

dx.doi.org/10.1021/jm301116j | J. Med. Chem. 2013, 56, 417−426

pharmacological target. Additionally, this differential affinity for biomembranes with different charge might contribute to understanding the higher activity and higher drug's penetration in Gram-positive bacteria compared with Gram-negative bacteria. The membrane location studies revealed that RFB is able to penetrate both membrane models. Indeed, the high partition and the deep location of RFB into the DMPC bilayer are suggestive of the drug's potential in vivo penetration into biological membranes.[38] The results obtained support the drug's wide distribution through the human body. Moreover, they contribute to our understanding of some of the toxicological effects, which are related to the RFB−membrane tropism and the ability to reach the body fluids and some of the most ordered membranes in the human body such as the epiretinal membrane.[39] The drug affects the biophysical parameters of membranes, namely the cooperativity, the lipid's order, and the fluid phase of both models. In particular, the drug causes a higher perturbation of these biophysical parameters in the negatively charged membrane model, with a noticeable increase of the order parameter in the fluid phase. The lipid's order increment indicates that the presence of the drug is responsible for higher phospholipid packing. This is consistent with the higher partition of RFB and its preferential location in the region nearer to the membrane surface, which might be translated in more pronounced effects in the biophysical parameters of the bacterial membrane. These data provide evidence that after the adsorption to the membrane interface via electrostatic interactions, RFB molecules undergo full immersion into the hydrophobic core. The zwitterionic contribution of RFB should be inserted according to its hydrophobicity gradient. In the human membrane, the hydrophilic part of RFB, namely imidazole and piperidine moieties, should therefore be located in the glycerol backbone and the hydrophobic naphthol should be incorporated at the phospholipid tails.[11] In the bacterial membrane model and because the positively charged contribution of RFB molecules are due to the protonated piperidine, the drug molecules establish stronger electrostatic interactions with the phosphate group of the DMPG, which explain the higher partition and the preferential surface location of RFB in the negatively charged model.

The results gathered suggest that the interactions of RFB with the bacterial membranes are mediated by electrostatic interactions, which might be a key to understand and to complement the knowledge about its mechanism of action. In fact, the mechanism by which RFB permeates through the bacterial membrane bilayer may include electrostatic adsorption. As the drug permeates through the membrane in direction to the RNA polymerase located inside of the bacterial cell, the location of the drug in the phospholipid membrane is responsible for a differential destabilization of the membranes. The RFB anchored to the head groups in the ordered region of the phospholipid membrane perturbs the phospholipid packing in the bacteria membrane. This closer lipid packing and therefore more restricted lateral movement might increase the susceptibility of the bacterial membrane to the oxidation of the membrane due to the action of the free radicals inside the macrophages, leading to the inhibition/killing of the bacteria.[40−42] Moreover, the influx/efflux of ions and nutrients trough the bacterial membrane might be compromised. Nevertheless, the human plasma membrane is much less disturbed due to a deeper insertion of the drug within the bilayer.

In conclusion, these findings represent a contribution to the medicinal chemistry field and permit to understand the differential interaction of RFB with membranes of different charge, which are putatively related to the therapeutic and toxic effects of this antibiotic and should therefore be taken into consideration when developing new RFB analogues for anti-TB therapy.

EXPERIMENTAL SECTION

Reagents and Equipment. The lipids (DMPC and DMPG) and *N*-(2-hydroxyethyl)piperazine-*N*′-(2-ethanesulfonic acid) (HEPES) were purchased from Sigma-Aldrich Co. (St. Louis, MO, USA). The probes, DPH and DPH-PA,were obtained from Molecular Probes (Invitrogen, Paisley, UK) and all were used as supplied. RFB was isolated from Mycobutin (Pfizer, Inc., New York) and further purified as described previously.[2] All other chemicals were supplied from Merck (Darmstadt, Germany). RFB's stock solutions were prepared in buffer:ethanol (9:1, v/v). The buffer HEPES 0.01 M (pH 7.4) was prepared with double-deionized water (conductivity less than 0.1 μS cm^{-1}) from a Millipore system, and the ionic strength (I = 0.1 M) was adjusted with NaCl.

Spectrophotometric measurements: the absorption spectra were recorded using a Perkin−Elmer Lambda 45 UV−Vis spectrophotometer, using quartz cells with a 1 cm^{-1} path length and a spectral range from 250 to 600 at 1 nm intervals.

Fluorescence measurements: fluorimetric data were collected using a Perkin−Elmer LS 50 B steady-state fluorescence spectrometer equipped with a constant-temperature cell holder. All data were recorded with excitation and emission slits between 2.5 and 3.0 nm. The excitation wavelength was set to 357 nm for DPH and 360 nm for DPH-PA. The emission wavelength was set to 427 nm for DPH and 430 nm for DPH-PA. All fluorescence intensity data were corrected for the quencher absorbance at the excitation wavelength.[43]

Fluorescence lifetime measurements: modulation frequencies were acquired between 10 and 200 MHz in a Fluorolog Tau-3 Lifetime spectrofluorimeter. Integration time was 10 s. Manual slits were of 0.5 mm, slits for monochromator excitation were of 7 mm (side entrance) and 0.7 mm (side exit) and for monochromator emission of 7 mm (side entrance) and 7 mm (side exit). The fluorescence emission was detected with a 90° scattering geometry. All measurements were made using Ludox as a reference standard (τ = 0.00 ns).

Anisotropy measurements: the fluorescence anisotropy was measured with a Jasco FP-6500 spectrofluorometer (Jasco, Great Dunmow, UK) equipped with two polarizers in the paths for excitation and emission using the L-format method. Samples with DPH and DPH-PA were heated in a range of 10 to 40 °C at the same wavelengths used for the fluorescence measurements.

Experimental Methods. *Preparation of Liposomes.* A lipid film was formed from a chloroform solution of lipids, dried under a stream of nitrogen, and left under reduced pressure for a minimum of 45 min to remove all traces of the organic solvent. Liposomes were prepared by the addition of the buffer system, followed by vortexing to yield multilamellar vesicles (MLVs). Lipid suspensions were equilibrated at 37.0 ± 0.1 °C for 30 min and extruded 10 times through polycarbonate filters with a pore diameter of 100 nm to form LUVs.[14] To prepare the fluorescence labeled liposomes, the probes (DPH or DPH-PA) were dissolved in chloroform/methanol and added to the lipid to give a probe:lipid molar ratio of 1:300, followed by a 30 min incubation period in the dark.[21,44,45]

Determination of Partition Coefficients by Derivative Spectrophotometry. The partition coefficient (K_p) of RFB between LUVs suspensions of DMPC or DMPG and aqueous solution (HEPES: 0.01 M, I = 0.1 M, pH 7.4) was determined by derivative spectrophotometry. In the derivative spectrophotometric studies, a series of buffered suspensions containing a fixed concentration of RFB (25 μM) and increasing concentrations of DMPC or DMPG (50, 100, 200, 300, 400, 500, 700, 900, 1000 μM) were prepared. The corresponding reference solutions were identically prepared but without the drug. All

suspensions were then vortexed and incubated in the dark at 37.0 ± 0.1 °C for 30 min.

Membrane Location Studies by Fluorescence Quenching. The drug's location within the membrane models were performed using steady-state fluorescence and lifetime fluorescence measurements of DPH and DPH-PA fluorophore probes in liposome buffered suspensions prepared with DMPC and DMPG at pH 7.4 (HEPES: 0.01 M, I = 0.1 M, pH 7.4). Buffer solutions of RFB were added to liposomes labeled with the probes, and the resulting suspensions were incubated in the dark at 37.0 ± 0.1 °C for 30 min. The studies were made according to an already described method[21] and consisted of the incubation of increasing amounts of drug (0−27 μM) with DMPC and DMPG liposomes at 37.0 ± 0.1 °C for 30 min while maintaining the total lipid concentration constant (500 μM).

Membrane Fluidity Studies. The effect of RFB (30 μM) on membrane microviscosity was evaluated by steady-state anisotropy measurements using LUVs of DMPC and DMPG (500 μM) labeled with DPH and DPH-PA probes as previously described.[21] The anisotropy values were recorded at several temperatures between 10 and 40 °C, with an accuracy of 0.1 °C. The order parameter was calculated in the fluid phase for both lipids.

Computational Methods. The chemical software used to predict the charge of RFB in bulk solution (pH 7.4) and to the octanol/water log P and log D was the MarvinView 5.4.1.1 software from ChemAxon.

AUTHOR INFORMATION

Corresponding Author

*Phone: +351-220428672. Fax: +351-226093483. E-mail: shreis@ff.up.pt.

Notes

The authors declare no competing financial interest.

ACKNOWLEDGMENTS

Marina Pinheiro and João M. Caio thank FCT (Lisbon) for the doctoral fellowships (SFRH/BD/63318/2009 and SFRH/BD/66789/2009, respectively). Cláudia Nunes thanks FCT (Lisbon) for the postdoctoral fellowship (SFRH/BPD/81963/2011). We are also grateful to the FCT for financial support under projects PEst-OE/QUI/UI0612/2011 and PTDC/QUI-QUI/101022/2008 with coparticipation European Community funds from the FEDER, QREN, and COMPET.

ABBREVIATIONS USED

CL, cardiolipin; DMPC, 1,2-dimyristoyl-*sn*-glycero-phosphocholine; DMPG, 1,2-dimyristoyl-*sn*-glycero-3-phosphoglycerol; DPH, 1,6-diphenyl-1,3,5-hexatriene; DPH-PA, (2-carboxyethyl)-1,6-diphenyl-1,3,5-hexatriene; HEPES, *N*-(2-hydroxyethyl) piperazine-*N*′-(2-ethanesulfonic acid); LUVs, Large unilamellar vesicles; MLVs, multilamellar vesicles; RFB, Rifabutin; TB, tuberculosis; T_m, main phase transition temperature

REFERENCES

(1) Aristoff, P. A.; Garcia, G. A.; Kirchhoff, P. D.; Hollis Showalter, H. D. Rifamycins—obstacles and opportunities. *Tuberculosis* **2010**, *90*, 94−118.

(2) Figueiredo, R.; Moiteiro, C.; Medeiros, M. A.; da Silva, P. A.; Ramos, D.; Spies, F.; Ribeiro, M. O.; Lourenco, M. C.; Junior, I. N.; Gaspar, M. M.; Cruz, M. E.; Curto, M. J.; Franzblau, S. G.; Orozco, H.; Aguilar, D.; Hernandez-Pando, R.; Costa, M. C. Synthesis and evaluation of rifabutin analogs against *Mycobacterium avium* and H(37)Rv, MDR, and NRP *Mycobacterium tuberculosis*. *Bioorg. Med. Chem.* **2009**, *17*, 503−511.

(3) Gaspar, M.; Neves, S.; Portaels, F.; Pedrosa, J.; Silva, M.; Cruz, M. Therapeutic efficacy of lipossomal rifabutin in a *Mycobacterium avium* model of infection. *Antimicrob. Agents Chemother.* **2000**, *44*, 2424−2430.

(4) Sousa, M.; Pozniak, A.; Boffito, M. Pharmacokinetics and pharmacodynamics of drug interactions involving rifampicin, rifabutin, and antimalarial drugs. *J Antimicrob Chemother.* **2008**, *62*, 872−878.

(5) Gisbert, J. P.; Calvet, X. Review article: rifabutin in the treatment of refractory *Helicobacter pylori* infection. *Aliment. Pharmacol. Ther.* **2012**, *35*, 209−221.

(6) Lucio, M.; Lima, J. L.; Reis, S. Drug−membrane interactions: significance for medicinal chemistry. *Curr. Med. Chem.* **2010**, *17*, 1795−1809.

(7) Vollhardt, D.; Fainerman, V. B. Characterisation of phase transition in adsorbed monolayers at the air/water interface. *Adv. Colloid Interface Sci.* **2010**, *154*, 1−19.

(8) Lintker, K. B.; Kpere-Daibo, P.; Fliesler, S. J.; Serfis, A. B. A comparison of the packing behavior of egg phosphatidylcholine with cholesterol and biogenically related sterols in Langmuir monolayer films. *Chem. Phys. Lipids* **2009**, *161*, 22−31.

(9) Bernardo, M. A.; Pina, F.; Garcia-Espana, E.; Latorre, J.; Luis, S. V.; Llinares, J. M.; Ramirez, J. A.; Soriano, C. Thermodynamic and Steady-State Fluorescence Emission Studies on Metal Complexes of Receptors Containing Benzene Subunits. *Inorg Chem.* **1998**, *37*, 3935−3942.

(10) Komath, S. S.; Kenoth, R.; Swamy, M. J. Thermodynamic analysis of saccharide binding to snake gourd (*Trichosanthes anguina*) seed lectin. Fluorescence and absorption spectroscopic studies. *Eur. J. Biochem.* **2001**, *268*, 111−119.

(11) Vostrikov, V. V.; Selishcheva, A. A.; Sorokoumova, G. M.; Shakina, Y. N.; Shvets, V. I.; Savel'ev, O. Y.; Polshakov, V. I. Distribution coefficient of rifabutin in liposome/water system as measured by different methods. *Eur. J. Pharm. Biopharm.* **2008**, *68*, 400−405.

(12) Vostrikov, V. V.; Selishcheva, A. A.; Sorokoumova, G. M.; Shvets, V. I. Determination of the distribution coefficient of rifabutin by the fluorescence study in the system liposome−water. *Biofizika.* **2007**, *52*, 521−526.

(13) Merino, S.; Vazquez, J. L.; Domènech, Ò.; Berlanga, M.; Vinãs, M.; Montero, M. T.; Hernández-Borrell, J. Fluoroquinolone−Biomembrane Interaction at the DPPC/PG Lipid−Bilayer Interface. *Langmuir* **2002**, *18*, 3288−3292.

(14) Pereira-Leite, C.; Nunes, C.; Lima, J. L.; Reis, S.; Lucio, M. Interaction of celecoxib with membranes: the role of membrane biophysics on its therapeutic and toxic effects. *J. Phys. Chem. B* **2012**, *116*, 13608−13617.

(15) Alves, I. D.; Goasdoue, N.; Correia, I.; Aubry, S.; Galanth, C.; Sagan, S.; Lavielle, S.; Chassaing, G. Membrane interaction and perturbation mechanisms induced by two cationic cell penetrating peptides with distinct charge distribution. *Biochim. Biophys. Acta* **2008**, *1780*, 948−959.

(16) Raquel, E.; Richard, E. Functional Consequences of the Lateral Organization of Biological Membranes. In *The Structure of Biological Membranes*, 3rd ed.; Yeagle, L. P., Ed.; CRC Press: New York, 2011; pp 133−152.

(17) Shakina, Y. N.; Vostrikov, V. V.; Sorokoumova, G. M.; Selishcheva, A. A.; Shvets, V. I. Interaction of rifabutin with model membranes. *Bull. Exp. Biol. Med.* **2005**, *140*, 711−713.

(18) Ferreira, H.; Lucio, M.; de Castro, B.; Gameiro, P.; Lima, J. L.; Reis, S. Partition and location of nimesulide in EPC liposomes: a spectrophotometric and fluorescence study. *Anal. Bioanal. Chem.* **2003**, *377*, 293−298.

(19) Henzing, A. J.; Dodson, H.; Reid, J. M.; Kaufmann, S. H.; Baxter, R. L.; Earnshaw, W. C. Synthesis of novel caspase inhibitors for characterization of the active caspase proteome in vitro and in vivo. *J. Med. Chem.* **2006**, *49*, 7636−7645.

(20) Connell, N. D.; Nikaido, H. Membrane Permeability and Transport in *Mycobacterium tuberculosis*. In *The Tuberculosis: Pathogenesis, Protection, and Control*, 1st ed.; Bloom, B., Ed.; ASM Press: Washington DC, 1994; pp 340.

(21) Brittes, J.; Lucio, M.; Nunes, C.; Lima, J. L.; Reis, S. Effects of resveratrol on membrane biophysical properties: relevance for its pharmacological effects. *Chem. Phys. Lipids* **2010**, *163*, 747−754.

(22) Grumetto, L.; Carpentiero, C.; Barbato, F. Lipophilic and electrostatic forces encoded in IAM-HPLC indexes of basic drugs: Their role in membrane partition and their relationships with BBB passage data. *Eur. J. Pharm. Sci.* **2012**, *45*, 685−692.
(23) Eftink, R. M. Fluorescence Quenching: Theory and Applications. In *The Principles of Fluorescence Spectroscopy*, 3rd ed.; Lakowicz, J. R., Ed.; Springer: New York, 2006; pp 53−120.
(24) Cardoso, A. M. S.; Faneca, H.; Almeida, J. o. A. S.; Pais, A. A. C. C.; Marques, E. F.; de Lima, M. C. P.; Jurado, A. l. S. Gemini surfactant dimethylene-1,2-bis(tetradecyldimethylammonium bromide)-based gene vectors: a biophysical approach to transfection efficiency. *Biochim. Biophys. Acta, Biomembr.* **2011**, *1808*, 341−351.
(25) Kaiser, R. D.; London, E. Location of Diphenylhexatriene (DPH) and Its Derivatives within Membranes: A Comparison of Different Fluorescence Quenching Analyses of Membrane Depth. *Biochemistry* **1998**, *37*, 8180−8190.
(26) Monteiro, J.; Videira, R.; Matos, M.; Dinis, A.; Jurado, A. Non-Selective Toxicological Effects of the Insect Juvenile Hormone Analogue Methoprene. A Membrane Biophysical Approach. *Appl. Biochem. Biotechnol.* **2008**, *150*, 243−257.
(27) Lucio, M.; Ferreira, H.; Lima, J. L.; Reis, S. Use of liposomes to evaluate the role of membrane interactions on antioxidant activity. *Anal. Chim. Acta* **2007**, *597*, 163−170.
(28) Castanho, M. A.; Prieto, M. J. Fluorescence quenching data interpretation in biological systems. The use of microscopic models for data analysis and interpretation of complex systems. *Biochim. Biophys. Acta* **1998**, *1373*, 1−16.
(29) Weeraman, C.; Chen, M.; Moffatt, D. J.; Lausten, R.; Stolow, A.; Johnston, L. J. A combined vibrational sum frequency generation spectroscopy and atomic force microscopy study of sphingomyelin-cholesterol monolayers. *Langmuir* **2012**, *28*, 12999−13007.
(30) Grancelli, A.; Morros, A.; Cabanas, M. E.; Domenech, O.; Merino, S.; Vazquez, J. L.; Montero, M. T.; Vinas, M.; Hernandez-Borrell, J. Interaction of 6-fluoroquinolones with dipalmitoylphosphatidylcholine monolayers and liposomes. *Langmuir* **2002**, *18*, 9177−9182.
(31) Lucio, M.; Ferreira, H.; Lima, J. L.; Reis, S. Interactions between oxicams and membrane bilayers: an explanation for their different COX selectivity. *Med Chem.* **2006**, *2*, 447−456.
(32) John, K.; Kubelt, J.; Muller, P.; Wustner, D.; Herrmann, A. Rapid transbilayer movement of the fluorescent sterol dehydroergosterol in lipid membranes. *Biophys. J.* **2002**, *83*, 1525−1534.
(33) Riske, K. A.; Fernandez, R. M.; Nascimento, O. R.; Bales, B. L.; Lamy-Freund, M. T. DMPG gel−fluid thermal transition monitored by a phospholipid spin labeled at the acyl chain end. *Chem. Phys. Lipids* **2003**, *124*, 69−80.
(34) Lipp, M. M.; Lee, K. Y.; Waring, A.; Zasadzinski, J. A. Fluorescence, polarized fluorescence, and Brewster angle microscopy of palmitic acid and lung surfactant protein B monolayers. *Biophys. J.* **1997**, *72*, 2783−2804.
(35) Nunes, C.; Brezesinski, G.; Pereira-Leite, C.; Lima, J. L.; Reis, S.; Lucio, M. NSAIDs interactions with membranes: a biophysical approach. *Langmuir* **2011**, *27*, 10847−10858.
(36) Rodrigues, C.; Gameiro, P.; Prieto, M.; Castro, B. Interaction of rifampicin and isoniazid with large unilamellar liposomes: spectroscopic location studies. *Biochim. Biophys. Acta* **2003**, *1620*, 151−159.
(37) Kohanski, M. A.; Dwyer, D. J.; Collins, J. J. How antibiotics kill bacteria: from targets to networks. *Nature Rev. Microbiol.* **2010**, *8*, 423−435.
(38) Pinheiro, M.; Lucio, M.; Reis, S.; Lima, J. L.; Caio, J. M.; Moiteiro, C.; Martin-Romero, M. T.; Camacho, L.; Giner-Casares, J. J. Molecular interaction of rifabutin on model lung surfactant monolayers. *J. Phys. Chem. B* **2012**, *116*, 11635−11645.
(39) Borchman, D.; Yappert, M. C. Lipids and the ocular lens. *J. Lipid Res.* **2010**, *51*, 2473−2488.
(40) Mowri, H.; Nojima, S.; Inoue, K. Effect of lipid composition of liposomes on their sensitivity to peroxidation. *J. Biochem.* **1984**, *95*, 551−558.
(41) Parker, A.; Miles, K.; Cheng, K. H.; Huang, J. Lateral distribution of cholesterol in dioleoylphosphatidylcholine lipid bilayers: cholesterol−phospholipid interactions at high cholesterol limit. *Biophys. J.* **2004**, *86*, 1532−1544.
(42) Huang, J. Model membrane thermodynamics and lateral distribution of cholesterol: from experimental data to Monte Carlo simulation. *Methods Enzymol.* **2009**, *455*, 329−364.
(43) Sweeney, L. G.; Wang, Z.; Loebenberg, R.; Wong, J. P.; Lange, C. F.; Finlay, W. H. Spray-freeze-dried liposomal ciprofloxacin powder for inhaled aerosol drug delivery. *Int. J. Pharm.* **2005**, *305*, 180−185.
(44) Lúcio, M.; Nunes, C.; Gaspar, D.; Golebska, K.; Wisniewski, M.; Lima, J. L. F. C.; Brezesinski, G.; Reis, S. Effect of anti-inflammatory drugs in phosphatidylcholine membranes: a fluorescence and calorimetric study. *Chem. Phys. Lett.* **2009**, *471*, 300−309.
(45) Nunes, C.; Brezesinski, G.; Lopes, D.; Lima, J. L.; Reis, S.; Lucio, M. Lipid−drug interaction: biophysical effects of tolmetin on membrane mimetic systems of different dimensionality. *J. Phys. Chem. B* **2011**, *115*, 12615−12623.